ADVANCED MATERIALS

DOI: 10.1002/adma.200800193

Core/Single-Crystal-Shell Nanospheres for Controlled Drug Release via a Magnetically Triggered Rupturing Mechanism**

By *Shang-Hsiu Hu, San-Yuan Chen,* Dean-Mo Liu,** and *Chi-Sheng Hsiao*

Recently, superparamagnetic iron oxide nanoparticles with enhanced functionality through surface modification or combination with functional materials have been widely used in a variety of biological applications such as drug or gene delivery,[1–4] bioseparation,[5,6] magnetic resonance imaging,[7–10] and hyperthermia therapy.[11] In contrast, there have been only a limited number of reports that addressed the use of magnetic nanoparticles for controlled drug delivery.[12,13] Most of the drug-containing magnetic nanocarriers comprise magnetic nanoparticulate ''cores'' with an organic or inorganic ''shell'', where therapeutic drugs are encapsulated within the shell structure. Drug release from these magnetic core/shell nanocarriers can easily be triggered by an external magnet, which has become known as the ''magnetic motor'' for site-specific drug delivery applications.[13] However, it is impossible to provide ''zero release'' capability before the drug-containing nanocarriers reach the target sites, because the thermodynamic nature of diffusion of drug molecules from the nanocarriers to the environment is virtually unavoidable in the presence of a drug concentration gradient.[12] Once triggered, the originally designed dose of drug for treating the targeted disease will be changed, sometimes in an unexpected manner, reducing the therapeutic efficiency. Therefore, a novel design for a nanocarrier that eliminates undesirable drug release before reaching the target site will be of interest and is practically desirable. In the meantime, it is more than critical that the drug can be released truly after reaching the target, in a controllable manner via external stimuli.

It is desirable that drug release behavior can be optimized and customized into a burst fashion, mimicking the natural release of biomolecules in the body.[14] Therefore, many studies have reported responses to specific stimuli, such as temperature,[15,16] pH,[17,18] electric fields,[19] mechanical signals,[20] ultrasound,[21,22] and magnetic fields[23–27] for controlled drug release applications. Magnetic fields provide a noncontact nature, which permits dosing that is remotely manageable, in comparison with those that require a physical or chemical contact to trigger drug release action on practical applications. However, nanoparticulate drug carriers with an accurate and fast response to a magnetic field have not been achieved. Here, we report a novel core/shell nanocarrier with a drug-containing silica core surrounded by a single-crystalline iron oxide shell. With such a unique core/shell configuration, we believe that biomolecules encapsulated in the core with an outer single-crystalline thin iron oxide shell can be protected from damage from harsh environments and, as one major objective of this study, eliminate uncontrollable release resulting from natural diffusion of molecules upon delivery in, for example, a patient's body. On the other hand, the magnetic nanoshell displays an ultrafast response and sensitivity upon exposure to a high-frequency magnetic field (HFMF), in which the highly magnetism-sensitive property of the nanometer-scale shell allows a controlled burst release of drug in a quantitative manner. In comparison, such a novel core/shell poly(vinyl pyrrolidone (PVP)-modified silica/Fe_3O_4 nanosphere is expected to provide much greater advantages in biomedical uses than existing alternatives.

The PVP-modified silica/Fe_3O_4 core/shell nanospheres shown in Figure 1a display a spherical geometry with a diameter ranging from 15 to 23 nm. The high-resolution transmission electron microscopy (HRTEM) image in Figure 1b confirms the core and shell nanostructure, which is clearly discernable with an amorphous silica core phase and a thin crystalline shell phase that completely encloses the core. No observable crevices or cracks are visually detectable at the interface of these core/shell nanospheres, suggesting excellent physical integrity between the two dissimilar phases. The thickness of the shell is about 4 nm on average, and the shell demonstrates a relatively dense, single-crystal nanoarchitecture with an orderly arranged crystal lattice clearly shown in the HRTEM image. The nanoshell crystal structure can be clearly identified as magnetite phase (Fe_3O_4). Such a highly ordered arrangement of the crystal lattice in the shell structure is relatively unique, and is suggested to be the result of self-assembly of the iron oxide salt in the presence of the PVP polymer.[28,29] Although the actual growth mechanism of the single-crystalline iron oxide shell is unclear at present, it is believed that with the adsorption of PVP on the surface of the silica cores, the iron ions can be efficiently anchored onto the pyrrolidone ring of PVP, which promotes an epitaxial-like growth of the oxide to form a

[*] Prof. S. Y. Chen, Prof. D. M. Liu, S. H. Hu, C. S. Hsiao
Department of Materials Sciences and Engineering
National Chiao Tung University
Hsinchu 300 (Taiwan)
E-mail: sanyuanchen@mail.nctu.edu.tw; deanmo_liu@yahoo.ca

[**] This work was financially supported by the National Science Council of the Republic of China, Taiwan under Contract No. NSC96-2627-B-009-006 and No. NSC96-2113-M009-027-MY2. We also thank Dr. C. H. Bow for TEM analysis. Supporting Information is available online from Wiley InterScience or from the authors.

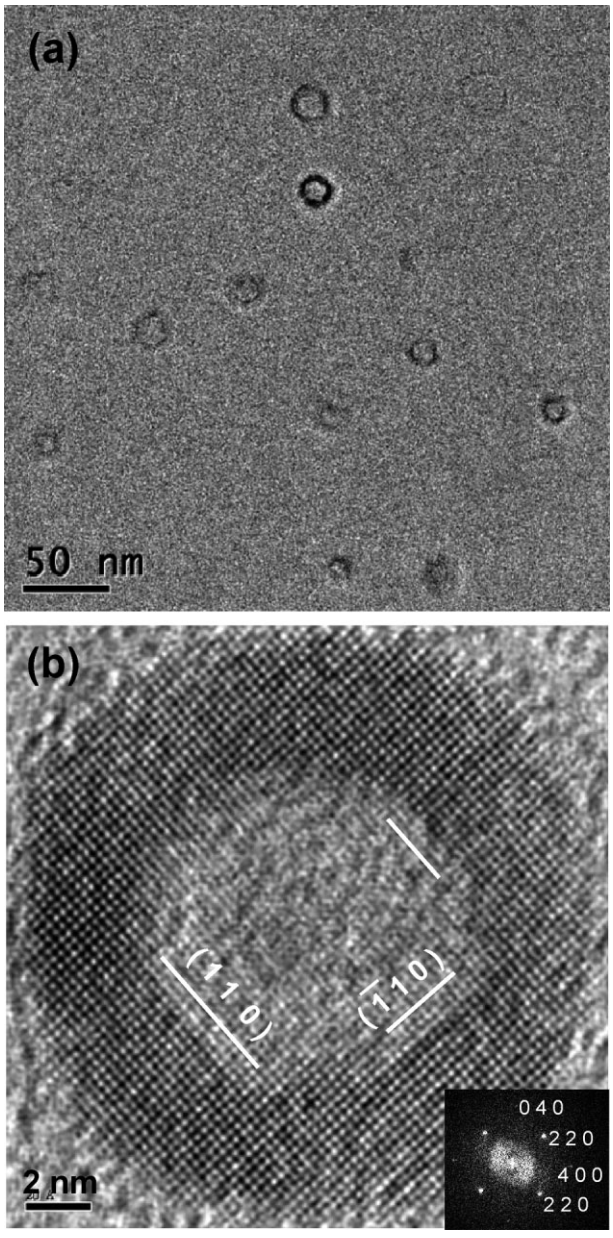

Figure 1. a) TEM image and b) HRTEM of PVP-modified silica/Fe_3O_4 core/shell nanospheres. Local Fourier transfer patterns indicate that the crystallographic structure is extremely uniform and homogenous throughout the shell. Some facet {1 1 0} planes are observed inside the nanosphere, and the Fourier transform pattern indicates that the shell is oriented at $z = [0\ 0\ 1]$.

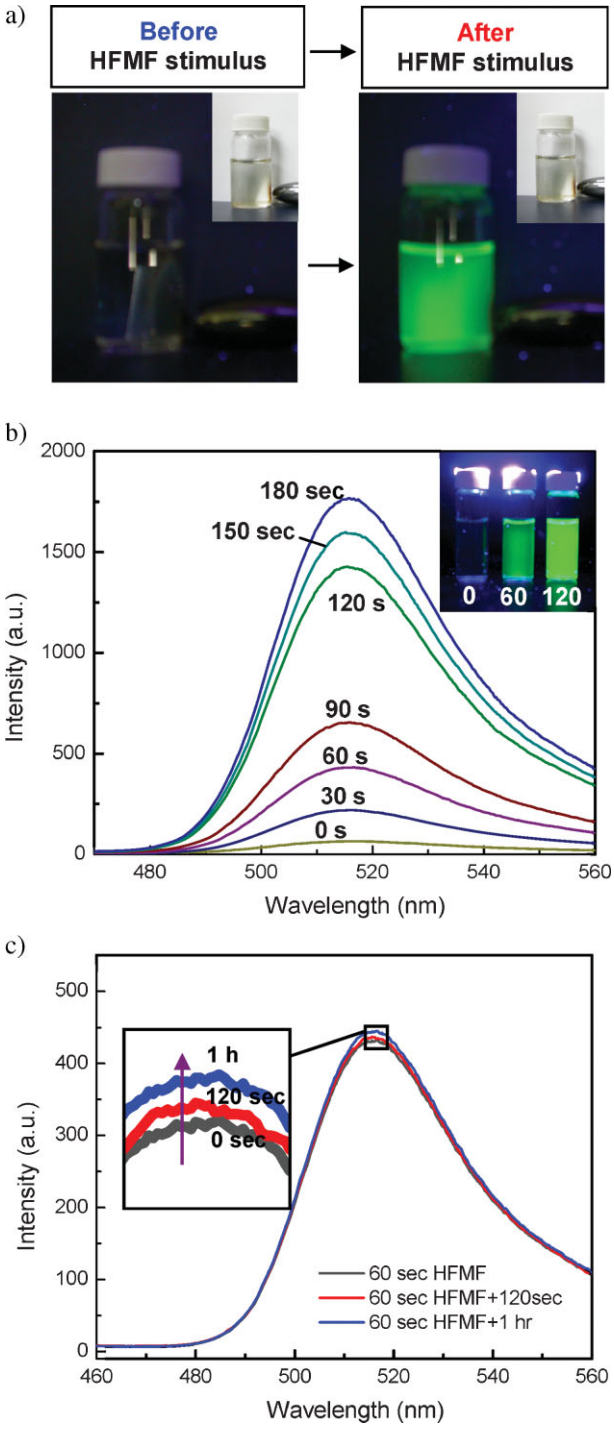

Figure 2. a) Photographs of the cuvettes with fluorescence-loaded PVP-modified silica/Fe_3O_4 core/shell nanospheres dispersed in water solution. Before HFMF exposure, fluorescence-loaded PVP-modified silica/Fe_3O_4 core/shell nanospheres displayed no sign of fluorescence under the UV light (left); after exposure, green fluorescence released from the PVP-modified silica/Fe_3O_4 core/shell nanospheres was clearly detected (right). b) Emission spectra of PVP-modified silica/Fe_3O_4 core/shell nanospheres (15 mg per 10 mL water) for applying a HFMF from 30 s to 180 s. c) Emission spectra of PVP-modified silica/Fe_3O_4 core/shell nanospheres. Inset: negligibly small amounts of dye molecule are being further released from the nanospheres for a time period of 120 s in the absence of stimulus.

single-crystal structure while increasing solution pH upon synthesis.

To demonstrate the release behavior of a fluorescence dye (encapsulated in the core phase as model molecule) from the core/shell nanospheres in a high frequency magnetic field, two cuvettes were charged with fluorescence-loaded nanospheres (100 mg each) dispersed in 15 mL water solution. After 24 hours (Fig. 2a, right), the nanospheres with the green dye

ADVANCED MATERIALS

showed no sign of release from the nanospheres under UV detection, suggesting that the dye molecules were enclosed in the silica cores and effectively inhibited from diffusion to the surrounding solution for a time period of 24 hours; such a time period is far longer than the time duration required for a metabolic operation in the healthy body. However, upon applying a HFMF (50 kHz and a power output of 15 W) to the cuvette for 5 minutes (Fig. 2a, left), a large amount of dye was detected in the water solution, indicating that the molecules were being released rapidly from the nanosphere under magnetic stimulus. This indicates that the core/shell nanospheres are highly sensitive to HFMF stimulus and show outstanding remote-controlled release behavior.

A kinetic analysis was performed using photoluminescence (PL) spectroscopy to monitor the release of dye molecules from the core/shell nanospheres for different time periods of HFMF exposure. Figure 2b shows the resulting PL spectra of the dye at different time periods, where the intensity of the fluorescence spectra increases with time of MF exposure, until a maximum at 180 seconds. After this maximum, no further increase in peak intensity was detected, indicating that the dye molecules were completely released from the nanospheres after being exposed to a HFMF for 180 seconds. Because the test monitored different time periods of on/off stimulation, the time-dependent peak intensity indicates that the dye was released only when the magnetic field was applied to the nanospheres, and that the release ceased right after removal of the field. This observation suggests that the action of magnetically driven drug release from the core/shell nanosphere is reversible.

However, to further verify the reversibility of the open–close nature of the magnetic shell, we performed a simple test following a 60 second HFMF exposure. After keeping the sample away from the field for another 120 seconds, the PL spectrum, shown in Figure 2c, showed only a negligible change in spectral intensity in comparison with the first test, that is, the same as the spectrum at 60 seconds of exposure, indicating no or a negligible amount of dye molecules being further released from the nanospheres for an additional time period of 120 seconds in the absence of the stimulus. This simple test indicates that the shell is being reversibly closed right after the field was removed and that the dye molecules were physically enclosed inside the core phase again, where uncontrollable diffusion is completely avoided.

Because the use of a HFMF is able to induce a vibration of the magnetic shell, it is conceivable that a short HFMF exposure of the core/shell nanospheres may induce a relatively small deformation of the shell structure and result in a reversible change of the nanostructure after the field is removed. However, it is also conceivable that an irreversible change in the nanostructure of the core/shell nanospheres may occur if the physical deformation is large enough to cause permanent damage to the shell structure upon a long-term HFMF exposure. To verify this concept, a nitrogen-adsorption measurement was performed in order to evaluate the subtle variation of the nanostructure upon longer-term HFMF stimulation. Figure 3 shows the resulting nitrogen adsorption spectra for the nanospheres before and after HFMF exposure for 20 minutes. The as-synthesized nanospheres have a specific surface area of 47 $m^2 g^{-1}$ and a total pore volume of 0.089 $cm^3 g^{-1}$, and a considerable increase in the surface area and total pore volume of the nanospheres to 61 $m^2 g^{-1}$ (increased by ca. 30%) and 0.127 $cm^3 g^{-1}$ (by ca. 40%), respectively, was detected after the long-term exposure, suggesting that the nanoporous structure of the nanospheres is changed irreversibly after long-term exposure to HFMF. Since the shell is a relatively dense, single-crystalline structure that covers the core surface, no accessible paths are available for nitrogen molecules (ca. 30 $Å^2$) to diffuse in, and it is thus reasonable to believe that the measured specific surface area and pore volume of the as-synthesized nanospheres is the pore nature of the agglomerates of the nanospheres, that is, the pore volume obtained is then a sum of the volume of interparticle voids rather than the pore properties within the nanospheres. In contrast, the increment in specific pore volume and surface area of the nanospheres after long-term field stimulation is highly likely to be a contribution from within the porous structure of the nanospheres. In other words, the shell was structurally deformed or damaged, by which defects developed and were accessible for the molecules to release out from. This increase in both surface area and pore volume may also result from the dissolution of the silica core, however, such a concern seems not feasible because the porosity of the silica core itself remained the same after the 20 minute exposure test. The change in pore parameters is different from what was previously observed, where the nanoporous structure remained nearly unchanged after 60 seconds of HFMF exposure, however, the test is a long exposure rather than the short exposure illustrated in Figure 2b.

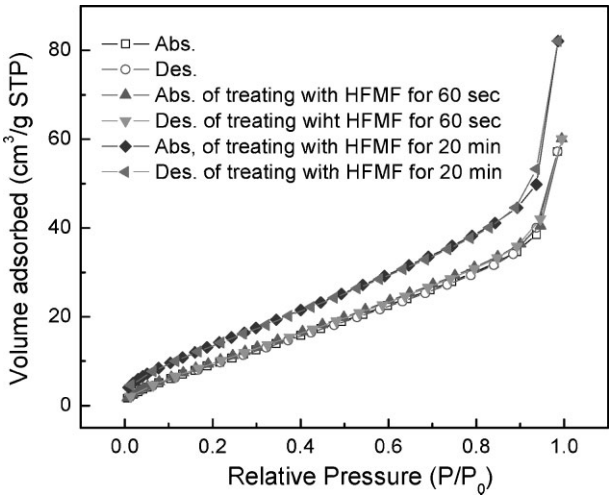

Figure 3. Nitrogen adsorption spectra for the nanospheres before and after 20 min of HFMF exposure. Brunauer–Emmett–Teller (BET) measurements of silica nanospheres treated with HFMF for 0 s, 60 s, and 20 min. STP: standard temperature and pressure.

To further elucidate the mechanism behind the release and zero-release behaviors, the nanospheres were examined using HRTEM after different time periods of stimulus, as illustrated in Figure 4, where a schematic drawing of the corresponding mechanism of controlled release is demonstrated. After a short exposure to the stimulus, that is, 60 seconds, the single-crystal nanoshell structure undergoes lattice deformation as a result of atomic rearrangement, forming a nanosized polycrystal of varying orientations. Boundaries between the nanopolycrystal are developed and it is highly likely that such boundaries (which are prone to develop nanocrevices under continuing stimulus) provide conduits for the dye molecules (that have dimensions estimated by software to be about 1.1. nm and a smallest height of only 0.1 nm) to be released. In other words, while being subjected to the magnetic field for a short-term period crevices or cracks of a nanometer scale were evolved along the boundary regions of the thin shell; magnetically induced vibrations enlarge the nanocrevices, permitting dye molecules to be released easily; and the change in the dimension of the nanocrevices is to a certain degree physically reversible upon short-term field exposure. However, following long-term exposure the nanocrevices are further enlarged to nanometer-scale cracks that propagate along the spherical shell structure and, ultimately, form irreversible deformations, that is, ruptures, of the shell when having absorbed sufficient amounts of the magnetic energy, resulting in an increase in both pore volume and surface area (Fig. 3).

The variation of the shell lattice structure from a single-crystalline configuration, that is, a single crystal, to formation of a polycrystal is seemingly physically irreversible, but the magnetism-sensitive behavior of these nanospheres appears to remain the same afterwards. This interesting phenomenon does offer great potential for developing a ''temporary single-crystal shell'' to protect and encapsulate molecules of interest more effectively for many types of specific delivery to diseased hosts without possible loss or damage of the molecules in the course of delivery. The variation of such a lattice change of the single-crystal iron oxide nanoshell upon magnetic stimulation may be a result of (a) thermally induced atomic rearrangement, where the free or surface energy of the single-crystal shell may be reduced by forming polycrystal of varying orientations, with some free or surface energy being reduced by formation of numerous inter-polycrystal boundaries; and (b) magnetically triggered mobility of the atoms along the direction of magnetization to reach a state of lower energy with enhanced structural stability, because the shell is essentially so thin and of such small dimensions that the surface energy should be relatively high and is structurally unstable.

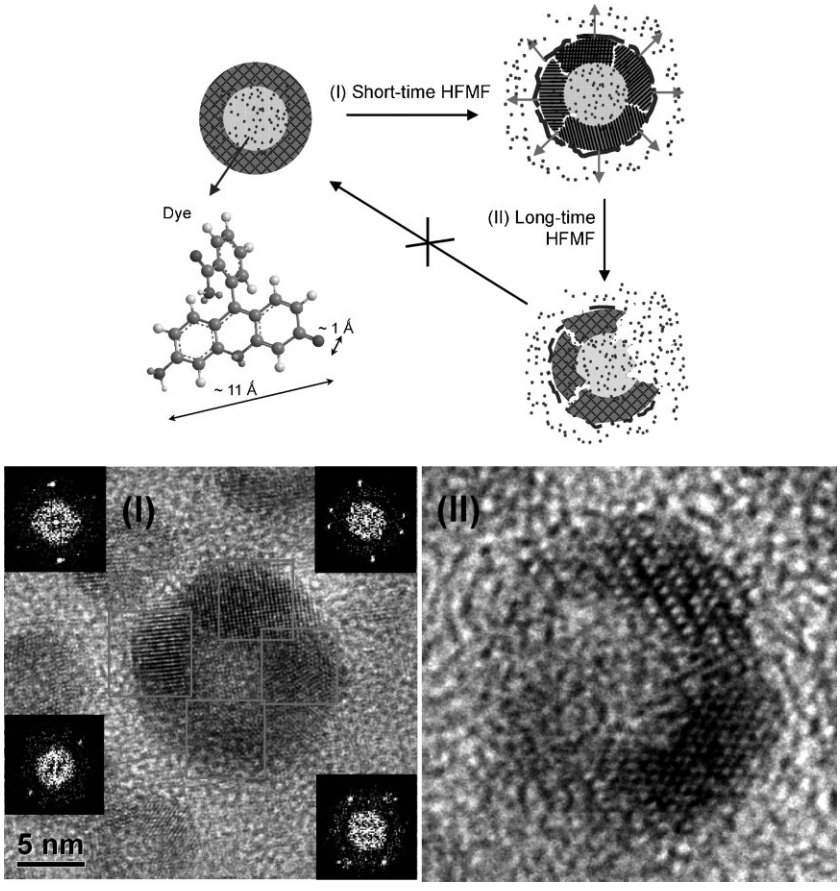

Figure 4. Schematic illustration of the thin shell with a proposed mechanism for controlled release of the fluorescence dye: (I) while applying HFMF, vibration enlarges the dimension of nanofaults, making it easy for dye molecules to be released. The change in the dimension of the nanofaults is physically reversible upon short-term field exposure. (II) Under long-term exposure, the nanofaults received sufficient amounts of (vigorous) energy (not specifically identified yet in this Communication), which permanently ruptures the thin shell.

Because the core/shell nanospheres are able to provide precise control of release and nonrelease characters for the molecules, which provides great advantages for drug delivery uses, it is, however, important to investigate the endocytosis following magnetically triggered drug release behavior of the nanodevice within cells. To further elucidate this behavior, HeLa (human cervical cancer) cells were incubated overnight with magnetic nanospheres loaded with green fluorescence dye to allow the endocytosis of nanospheres to be optically examined. Figure 5a shows optical and fluorescence microscopy images of the cell line before HFMF treatment, where a relatively weak green fluorescence is observed. However, after 30 seconds of HFMF stimulation, green fluorescence is clearly observed within the bodies of these HeLa cells upon excitation at 494 nm (Fig. 5b) which strongly indicates that the dye-loaded nanospheres were efficiently taken up by the cells and rapidly released the dyes within the cells in a

ADVANCED MATERIALS

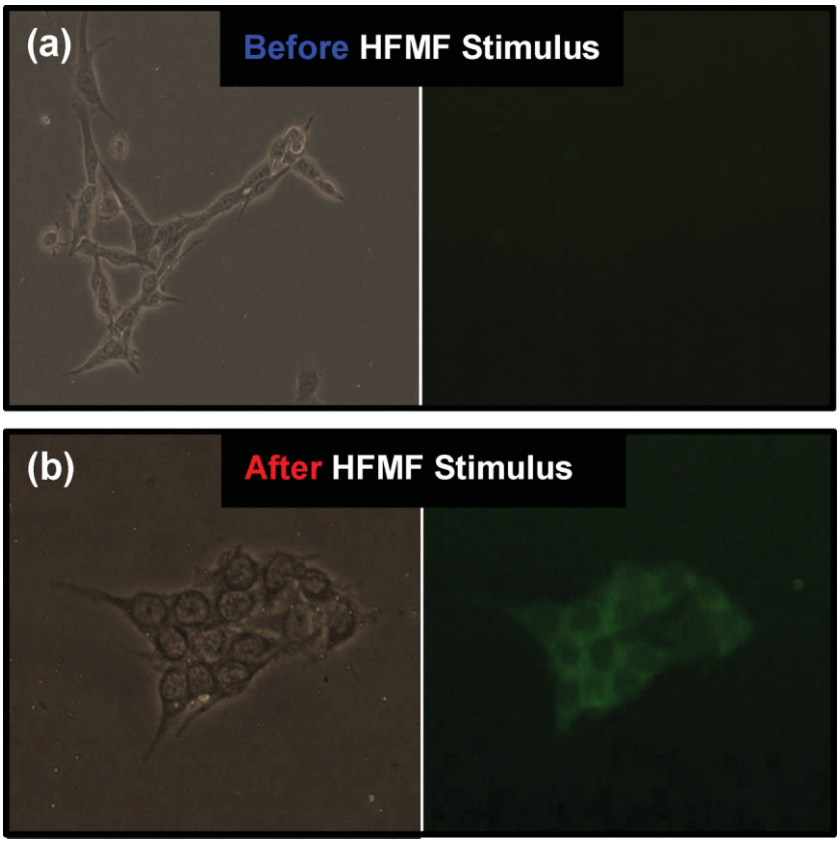

Figure 5. Fluorescence microscopy images of HeLa cells after 10 h incubation with fluorescence-loaded PVP-modified silica/Fe_3O_4 core/shell nanospheres. a) Without HFMF treatment, and b) after 30 s of HFMF stimulation, green fluorescence is clearly observed within the bodies of the HeLa cells upon excitation at 494 nm.

well-controllable manner. The dye molecules also illustrated well-controlled nonrelease behavior during the time period of the test. Therefore, we envision from the appearance of healthy, intact, fully grown cells that the nanospheres are biocompatible in vitro under experimental conditions, and precisely released the desirable molecule for therapeutic purposes.

In conclusion, we have demonstrated a novel core/shell nanosphere with a PVP-modified silica core followed by a functional deposition of a single-crystal iron oxide shell. Such a core/shell nanosphere offers surprisingly outstanding controlled release and nonrelease behavior for molecules encapsulated inside the silica core. The dense, single-crystalline shell is efficiently preventing the fluorescence dye from undesired release, given that an undesirable leakage of the molecule during the course of delivery is completely inhibited. Moreover, the molecules encapsulated in the core can be released in a highly controllable manner through the use of a magnetic stimulus. It is envisioned that the drug of interest can be released in a precise dosage in a remotely controlled manner or''burst'', with the shell being ruptured when the disease site is reached. We also envision from this study that these core/shell nanospheres are expected to play a significant role in the development of a new generation of site-specific controlled-release drug delivery nanodevices.

Experimental

A sol–gel process was used to encapsulate the fluorescence molecules within the silica matrix. First, 2 wt % PVP (0.06 mL; $M_w \sim 10000$) was dissolved in deionized (DI) water under stirring. 0.04 mL tetraethoxysilane (TEOS) was added into 25 mL ethanol, and 5 mL of 2 wt % PVP was mixed into the solution and preheated to 80 °C. Then, the fluorescence molecules were dissolved in the DI water, added into the solution, and mixed for 6 h. In a nitrogen atmosphere, 100 μL ammonia solution (33 wt %) was introduced to the prehydrolyzed TEOS solution. After 24 h, the ethanol was used to wash the silica nanoparticles to remove the surfactant and unreacted chemicals three times. The dye-loaded silica nanoparticles were dispersed in ethanol solution. Under nitrogen, $FeCl_3 \cdot 6H_2O$ and $FeCl_2 \cdot 4H_2O$ with a $FeCl_2/FeCl_3$ molar ratio of 2:1 were dissolved into water and then mixed with the PVP-modified silica nanoparticles with vigorous stirring at 80 °C under nitrogen atmosphere. After 4 h, the iron salts were adsorbed onto the PVP-modified silica nanoparticles, the ammonium water (33%) was slowly dripped into the mixed solution. Addition of 2 mL ammonium water (NH_4OH, 33%) caused precipitation, by which iron oxide shells were immediately formed on the surface of PVP-coated silica nanoparticles, forming a self-assembled core/shell nanosphere. The precipitated powders were collected through centrifugation at 6000 rpm, removed from the solution, and washed with DI water four times. The PVP-modified silica/Fe_3O_4 core/shell nanospheres were separated by centrifugation, and the average diameter of the core/shell nanospheres is about 20 nm.

The morphologies of the core/shell nanospheres were examined by using transmission electron microscopy (TEM, JEM-2010, Japan). X-ray diffractometry (XRD, M18XHF, Mac Science, Japan) was applied to identify the crystallographic phase of nanospheres, at a scanning rate of $2\theta = 6°$ min^{-1} over a 2θ range of 10° to 70°. The high-frequency magnetic field (HFMF) of 50–100 kHz was applied to the magnetic silica nanospheres to investigate the drug-release behavior. HFMF was set up from a power supply, functional generator, amplifier, and cooling water. Similar equipment has been reported elsewhere.[30] The strength of the magnetic field depended on the coils. In this study, the coil was 8 loops, the frequency was 50 kHz, and the strength of the magnetic field (H) was 2.5 kA m^{-1}. The temperature of the HFMF generator was controlled by cycling cooling water at 25 °C. The drug release behavior from the magnetic silica nanospheres was measured in 20 mL phosphate buffered saline per sponge cube (pH 7.4). PL spectroscopy (Fluorescence Spectrophotometer F-4500, Hitachi, Japan) was used to characterize the release profile of the dye molecules by measuring the change in the intensity of the fluorescence dye before and after a high-frequency magnetic field (HFMF) of 50 kHz was applied to the nanospheres dispersed in the water solution at a concentration of 0.01 wt % for time periods of 0, 30, 60, 90, 120, 150, to 180 s of HFMF exposure. BET analysis was measured using N_2 gas absorption isotherms at 77 K, and the BET surface areas were calculated in the region 0.05–0.3 of relative pressures.

HeLa (human cervical cancer) cells were maintained in Dulbecco's modified Eagle's medium (DMEM) containing 10% fetal bovine

serum, 100 units mL^{-1} penicillin, and 100 μg mL^{-1} streptomycin. Cells were cultured with complete medium at 37 °C in a humidified atmosphere of 5% CO_2 in air. The PVP-modified silica/Fe_3O_4 core/shell nanospheres were incubated with the cells for 12 h. Then, the cells were subjected to a HFMF for 0 and 60 s and observed by PL microscopy.

Received: January 21, 2008
Revised: March 3, 2008
Published online: June 2, 2008

[1] T. Neuberger, B. Schöpf, H. Hofmann, M. Hofmann, B. Rechenberg, *J. Magn. Magn. Mater.* **2005**, *293*, 483.
[2] M. Arruebo, M. Galán, N. Navascués, C. Téllez, C. Marquina, M. R. Ibarra, J. Santamaría, *Chem. Mater.* **2006**, *18*, 1911.
[3] N. Nasongkla, E. Bey, J. Ren, H. Ai, C. Khemtong, J. S. Guthi, S. F. Chin, A. D. Sherry, D. A. Boothman, J. Gao, *Nano Lett.* **2006**, *6*, 2427.
[4] N. Kohler, C. Sun, J. Wang, M. Zhang, *Langmuir* **2005**, *21*, 8858.
[5] P. S. Doyle, J. Bibette, A. Bancaud, J. L. Viovy, *Science* **2002**, *295*, 2237.
[6] I. Koh, X. Wang, B. Varughese, L. Isaacs, S. H. Ehrman, D. S. English, *J. Phys. Chem. B* **2006**, *110*, 1553.
[7] C. W. Lu, Y. Hung, J. K. Hsiao, M. Yao, T. H. Chung, Y. S. Lin, S. H. Wu, S. C. Hsu, H. M. Liu, C. Y. Mou, C. S. Yang, D. M. Huang, Y. C. Chen, *Nano Lett.* **2007**, *7*, 149.
[8] W. S. Seo, J. H. Lee, X. Sun, Y. Suzuki, D. Mann, Z. Liu, M. Terashima, P. C. Yang, M. V. Mcconnell, D. G. Nishimura, H. Dai, *Nat. Mater.* **2006**, *5*, 971.
[9] Y. M. Huh, Y. W. Jun, H. T. Song, S. Kim, J. S. Choi, J. H. Lee, S. Yoon, K. S. Kim, J. S. Shin, J. S. Suh, J. Cheon, *J. Am. Chem. Soc.* **2005**, *127*, 12387.
[10] O. Veiseh, C. Sun, J. Gunn, N. Kohler, P. Gabikian, D. Lee, N. Bhattarai, R. Ellenbogen, R. Sze, A. Hallahan, J. Olson, M. Zhang, *Nano Lett.* **2005**, *5*, 1003.
[11] A. Jordan, R. Scholz, P. Wust, H. Schirra, T. Schiestel, H. Schmidt, R. Felix, *J. Magn. Magn. Mater.* **1999**, *194*, 185.
[12] S. Giri, B. G. Trewyn, M. P. Stellmaker, V. S. Y. Lin, *Angew. Chem. Int. Ed.* **2005**, *44*, 5038.
[13] T. J. Yoon, J. S. Kim, B. G. Kim, K. N. Yu, M. H. Cho, J. K. Lee, *Angew. Chem. Int. Ed.* **2005**, *44*, 1068.
[14] A. C. R. Grayson, I. S. Choi, B. M. Tyler, P. P. Wang, H. Brem, M. J. Cima, R. Langer, *Nat. Mater.* **2003**, *2*, 767.
[15] Z. Hu, X. Xia, *Adv. Mater.* **2004**, *16*, 305.
[16] X. Z. Zhang, D. Q. Wu, C. C. Chu, *Biomaterials* **2004**, *25*, 3793.
[17] M. Das, S. Mardyani, W. C. W. Chan, E. Kumacheva, *Adv. Mater.* **2006**, *18*, 80.
[18] Y. Zhu, J. Shi, W. Shen, X. Dong, J. Feng, M. Ruan, Y. Li, *Angew. Chem. Int. Ed.* **2005**, *44*, 5083.
[19] M. R. Abidian, D. H. Kim, D. C. Martin, *Adv. Mater.* **2006**, *18*, 405.
[20] K. Y. Lee, M. C. Peters, D. J. Mooney, *Adv. Mater.* **2001**, *13*, 837.
[21] H. J. Kim, H. Matsuda, H. Zhou, I. Honma, *Adv. Mater.* **2006**, *18*, 3083.
[22] B. G. De Geest, A. G. Skirtach, A. A. Mamedov, A. A. Antipov, N. A. Kotov, S. C. De Smedt, G. B. Sukhorukov, *Small* **2007**, *3*, 804.
[23] J. Kost, J. Wolfrum, R. Langer, *J. Biomed. Mater. Res.* **1987**, *21*, 1367.
[24] E. R. Edelman, J. Kost, H. Bobeck, R. Langer, *J. Biomed. Mater. Res.* **1985**, *19*, 67.
[25] J. Kost, R. Noecker, E. Kunica, R. Langer, *J. Biomed. Mater. Res.* **1985**, *19*, 935.
[26] O. Saslawski, C. Weingarten, J. P. Benoit, P. Couvreur, *Life Sci.* **1988**, *42*, 1521.
[27] Z. Lu, M. D. Prouty, Z. Guo, V. O. Golub, C. S. S. R. Kumar, Y. M. Lvov, *Langmuir* **2005**, *21*, 2042.
[28] Y. Sun, Y. Yin, B. T. Mayers, T. Herricks, Y. Xia, *Chem. Mater.* **2002**, *14*, 4736.
[29] H. S. Qian, S. H. Yu, J. Y. Gong, L. B. Luo, L. F. Fei, *Langmuir* **2006**, *22*, 3830.
[30] R. Mohr, K. Kratz, T. Weigel, M. Lucka-Gabor, M. Moneke, A. Lendlein, *Proc. Natl. Acad. Sci. USA* **2006**, *103*, 3540.

